SUPPORTING INFORMATION

A targeted data-independent acquisition and mining strategy for trace drug metabolite identification using liquid chromatography coupled with tandem mass spectrometry

Yan Gao[†], Ruiping Zhang[†], Jinfa Bai[†], Xuejun Xia[§], Yanhua Chen[†], Zhigang Luo[†], Jing Xu [†], Yang Gao[†], Yuling Liu[§], Jiuming He[,†], and Zeper Abliz[*,†]*

[†]State Key Laboratory of Bioactive Substance and Function of Natural Medicines, Institute of Materia Medica, Chinese Academy of Medical Sciences and Peking Union Medical College, Beijing 100050, People's Republic of China
[§]Beijing Key Laboratory of Drug Delivery Technology and Novel Formulation, Institute of Materia Medica, Chinese Academy of Medical Sciences and Peking Union Medical College, Beijing 100050, People's Republic of China

CONTENTS

Methods **S-2**

Supplementary Tables and Figures **S-3**

Table S1. Six Templates of Molecular Ions and Fragment Ions for MF-MDFs **S-3**

Table S2. Potential Metabolites Identified by the TDIAM Strategy **S-4**

Figure S1. A comparison between tm-MS spectra of M2-M10 acquired by TDIAM and HRMS/MS spectra of M2-M10 ..... **S-4**

Figure S2. HRMS/MS spectra of the $[M+Na]^+$ ion at *m/z* 876.3207 for paclitaxel ... **S-6**

Scheme S1. Fragmentation reaction of the $[M+Na]^+$ ion of paclitaxel **S-7**

Figure S3. HRMS/MS spectra and proposed structures of M1–M10 ..... **S-8**

Supplementary References **S-9**

METHODS

Animal studies and sample collection. The metabolism study was approved by the Animal Care & Welfare Committee, Institute of Materia Medica, Chinese Academy of Medical Sciences and Peking Union Medical College, and was performed at the Animal Experimental Centre, Institute of Materia Medica. Female BALB/c-nu mice (No. 11400700053650) weighing 17 ± 1 g were obtained from Vital River Laboratories (Beijing, China) and provided with a certified standard mouse diet and water ad libitum. Temperature and relative humidity were controlled at 23 ± 5°C and 55 ± 5%, respectively, with a light cycle of 12 h on and 12 h off. After acclimatization for 3 days, mice were injected intravenously with paclitaxel at a dose of 20 mg kg^{-1}, and an equal volume of sterile saline was administered to the control group. Blood samples were collected into heparinized tubes at 0.5, 2, and 4 h after the saline or paclitaxel injection, and centrifuged at 1,000 rpm for 10 min at 4°C to separate plasma and red blood cells. Then, plasma samples were transferred into Eppendorf tubes and stored at -80°C pending sample preparation.

Chemicals and Reagents. Paclitaxel for injection (10 mL: 60 mg, Batch 130901) was purchased from Beijing Union Pharmaceutical Factory (Beijing, China). Paclitaxel analytical standards originated from the National Institutes for Food and Drug Control (NIFDC, Beijing, China). The 3'-hydroxypaclitaxel analytical standard was acquired from ChromaDex, Inc. (CA, USA). 6α-hydroxypaclitaxel and 6α, 3'-dihydroxypaclitaxel analytical standards were obtained from Toronto Research Chemicals Inc. (Toronto, Canada). HPLC-grade acetonitrile (ACN) and formic acid were purchased from Merck (Darmstadt, Germany), and other chemicals were of analytical grade.

Sample Preparation. Plasma sample volumes of 600 μL (a mixture of 200 μL plasma samples taken at 0.5 h, 1 h, and 2 h) were mixed with 1.8 mL cold ACN (4°C) in an Eppendorf tube. Each tube was vortexed for 3 min, and then centrifuged at 20,000 rpm for 10 min. The liquid phase was transferred to another tube, evaporated with nitrogen gas at 40°C, and then reconstituted with 100 μL of ACN/water (2:98, v/v). After vortexing for 5 min and centrifugation at 20,000 rpm for 2 min, the clean liquid phase was transferred to the autosampler in a glass vial with an insert, from which an aliquot of 5 μL was removed and injected for analysis.

UHPLC-HRMS/MS Conditions. The separation of the analytes from the plasma extract was carried out using a Dionex UltiMate 3000 UHPLC system, which consisted of an UltiMate 3000 RS pump, an UltiMate 3000 RS autosampler, and an UltiMate 3000 RS column compartment (Dionex, Olten/Switzerland). Gradient elution was performed on a separation column (Waters ACQUITY UPLC ® HSS column, 100 × 2.1mm id, 1.8 μm, Waters Corp.). The mobile phase consisted of 0.1% formic acid (eluent A) and ACN (eluent B), with linear gradient elution. Before starting each analysis, the UHPLC system was equilibrated for 8 min with a mixture of 98% eluent A and 2% eluent B. The gradient was programmed as follows: 0.00–9.00 min: gradient increased to 60% eluent B; 9.00–18.00 min: an isocratic step at 60% eluent B; 18.00–20.00 min: gradient increased to 100% eluent B; 20.00–27.00 min: another isocratic step at 100% eluent B; and 27.00 min: controller stopped. The flow

rate used was 0.25 mL min^{-1}. The UHPLC was coupled to a Q-Orbitrap mass spectrometer (QExactive, ThermoFisher Scientific) via a heated electrospray source (HESI), using the following operation parameters: sheath gas flow rate, 50; aux gas flow rate, 10; sweep gas flow rate, 0; spray voltage, 4 KV; capillary temperature, 380°C; S-lens RF level, 60; aux gas heater temperature, 300°C. High-purity nitrogen (N_2) was used as the nebulizing gas and the collision gas for HCD.

Blind Deconvolution. Blind deconvolution was used as a solution to get an automatic and reasonable 'purified' signal for co-eluting components from the overlapping chromatographic peaks. The mass peak deconvolution algorithm employed by home-modified ChemPattern was a fully improved variety of the model peak method[1,2]. The basic concept of the peak model method relies on recombining mass chromatograms related to individual components by calculating the match factor between each mass chromatogram of different *m/z* with the established peak model at a specific retention time.

As blind deconvolution involves many parameters, different parameters were examined for their influence on the process and the results: (1) Parsing parameters, including peak combination threshold, baseline determination threshold and total fragment ions detection, had a large influence on the result. Higher thresholds are predicted to yield more reliable results with a low misclassification rate. However, due to the rejection of uncertain ions, the rejection rate would also increase. (2) Precision parameters, including deconvolution S/N and ion peak tolerance, lead to a more precise result with a smaller residual at lower values, but result in lower deconvolution performance in terms of a longer calculation time and more memory consumption. (3) Filter parameters, including minimal peak area, addition and isotope ion combination, are not predicted to have an impact on the deconvolution procedure itself, but greatly affect the subsequent analysis procedure.

SUPPLEMENTARY TABLES AND FIGURES

Table S1. Six Templates of Molecular Ions and Fragment Ions for MF-MDFs.

Template	Molecular ion	Fragment ions				
	1	2	3	4	5	6
Template Mass (*m/z*)	876.3202	105.0337	308.0884	409.1611	531.1978	591.2186
ΔmDa Range (mDa)	±50	±50	±50	±50	±50	±50
Filter Start Mass (*m/z*)	600	50	200	350	400	500
Filter End Mass (*m/z*)	1300	200	400	500	700	700

Table S2. Potential Metabolites Identified by the TDIAM Strategy.

Peak ID	RT (min)	Putative Metabolite	Mass Shift	Molecular formula	Theo. *m/z*	Meas. *m/z*	ppm	New
P	12.22	Paclitaxel+Na	0.0000	$C_{47}H_{51}NO_{14}Na$	876.3202	876.3184	-2.0	
M1	10.81	Hydroxylation	15.9949	$C_{47}H_{51}NO_{15}Na$	892.3151	892.3183	3.6	
M2	11.07	Deacetylation	-42.0106	$C_{45}H_{49}NO_{13}Na$	834.3096	834.3118	2.6	
M3	11.09	Aliphatic hydroxylation	15.9949	$C_{47}H_{51}NO_{15}Na$	892.3151	892.3193	4.7	
M4	11.30	Dihydroxylation	31.9898	$C_{47}H_{51}NO_{16}Na$	908.3100	908.3125	2.7	Yes
M5	12.57	Hydroxylation	15.9949	$C_{47}H_{51}NO_{15}Na$	892.3151	892.3177	2.9	Yes
M6	12.63	Deacetylation and hydroxylation	-26.0151	$C_{45}H_{49}NO_{14}Na$	850.3051	850.3037	-1.6	Yes
M7	14.49	Dihydroxylation and dehydration and deacetylation	-28.0313	$C_{45}H_{47}NO_{14}Na$	848.2525	848.2538	1.5	Yes
M8	14.50	Hydroxylation	15.9949	$C_{47}H_{51}NO_{15}Na$	892.3151	892.3192	4.6	
M9	15.52	Hydroxylation and dehydration	-2.0157	$C_{47}H_{49}NO_{14}Na$	874.3045	874.3042	-0.4	Yes
M10	17.83	Dimethylation	28.0313	$C_{49}H_{55}NO_{14}Na$	904.3515	904.3516	0.1	Yes

Additional Performance Evaluation of TDIAM for M2–M10. Figure S1 shows that the tm-MS spectra of M2–M10 processed by MF-MDFs coupled with blind deconvolution were similar to HRMS/MS spectra of M2–M10 acquired by conventional MS/MS scan.

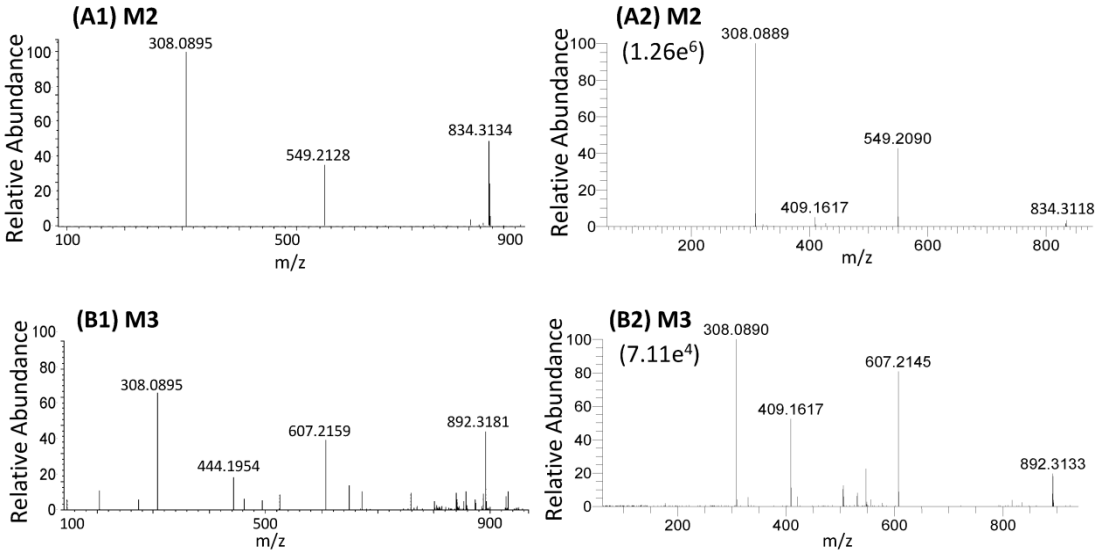

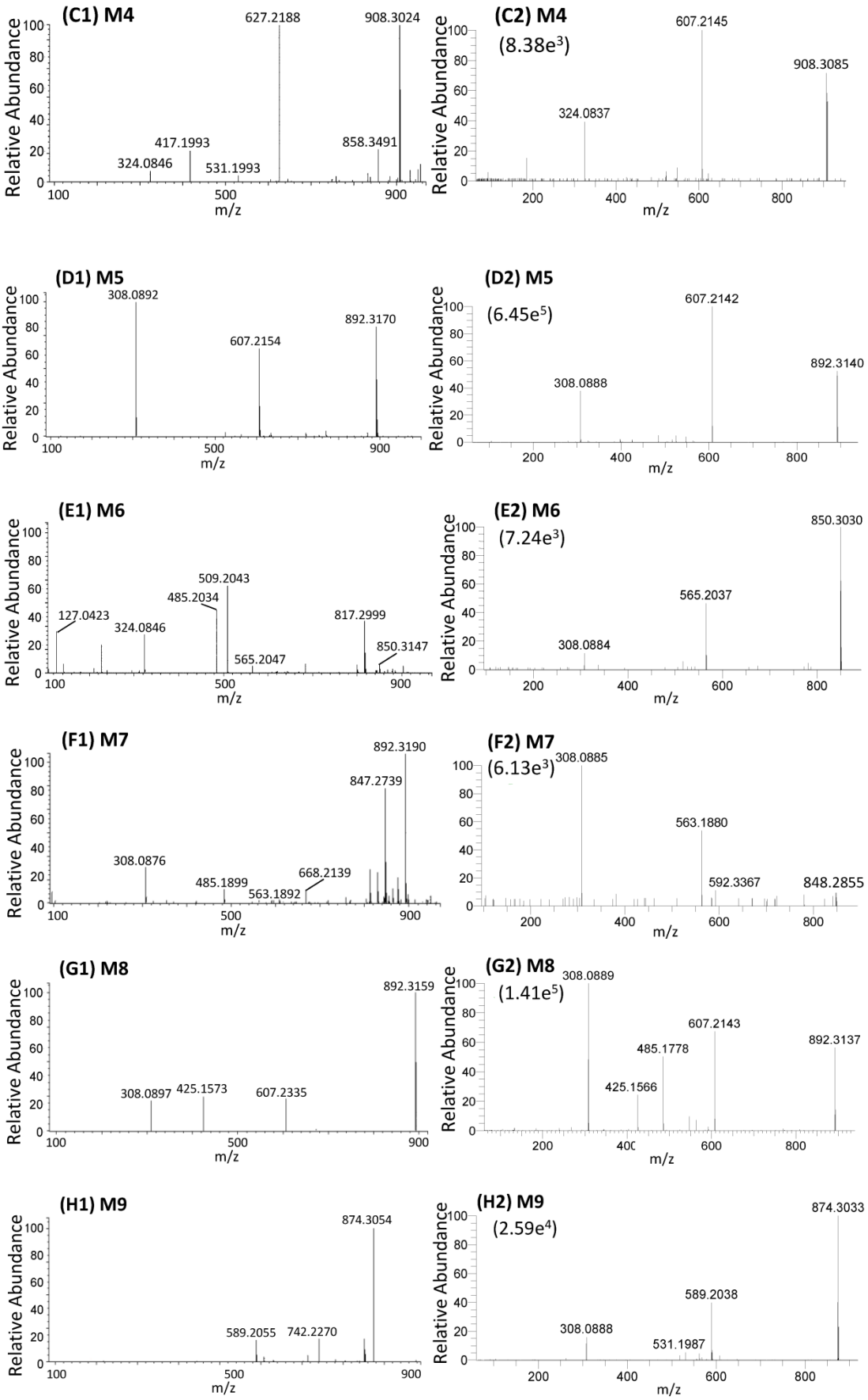
(C1) M4
627.2188
908.3024
417.1993
858.3491
324.0846
531.1993
(C2) M4
(8.38e3)
607.2145
908.3085
324.0837
(D1) M5
308.0892
892.3170
607.2154
(D2) M5
(6.45e5)
607.2142
892.3140
308.0888
(E1) M6
509.2043
485.2034
127.0423
324.0846
817.2999
850.3147
565.2047
(E2) M6
(7.24e3)
850.3030
565.2037
308.0884
(F1) M7
892.3190
847.2739
308.0876
668.2139
485.1899
563.1892
(F2) M7
(6.13e3)
308.0885
563.1880
592.3367
848.2855
(G1) M8
892.3159
308.0897
425.1573
607.2335
(G2) M8
(1.41e5)
308.0889
607.2143
485.1778
892.3137
425.1566
(H1) M9
874.3054
589.2055
742.2270
(H2) M9
(2.59e4)
874.3033
589.2038
308.0888
531.1987
Relative Abundance
m/z

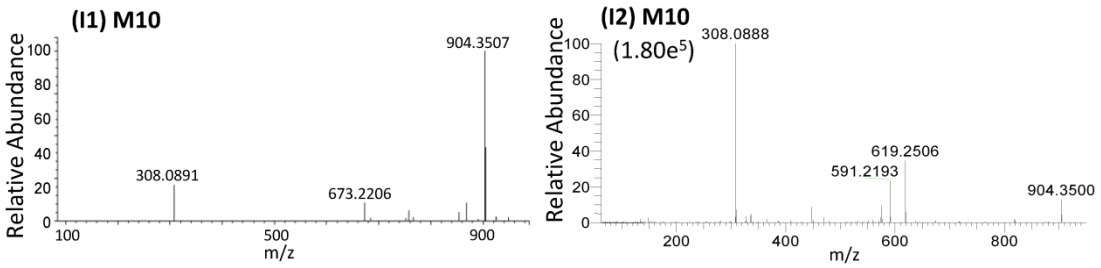

Figure S1. A comparison between tm-MS spectra of M2–M10 acquired by TDIAM and HRMS/MS spectra of M2–M10. Left: tm-MS spectra of M2–M10 processed by MF-MDFs coupled with blind deconvolution; Right: HRMS/MS spectra of M2–M10.

Fragmentation Behavior Investigation of Paclitaxel. Based on our previous investigation of structural features of taxoids revealed by FAB-MS/MS and ESI-MS/MS[3], an investigation of paclitaxel fragmentation was essential for data mining by a combination of MF-MDFs and deconvolution. In the HRMS and HRMS/MS spectrum of paclitaxel, an intense sodium adduct ion $[M+Na]^+$ (*m/z* 876.3207) (basic peak) was more abundant than the corresponding protonated molecular ion $[M+H]^+$ (*m/z* 854.3388), and formed fewer fragments, which were also sodium adduct ions. Three predominant product ions were $[ScH+Na]^+$ (*m/z* 308.0899), $[M+Na-ScH]^+$ (*m/z* 591.2206), and $[M+Na-ScH-HOAc]^+$ (*m/z* 531.1995) (formed by eliminating HOAc from $[M-ScH+Na]^+$ ion). The fragmentation reaction of the $[M+Na]^+$ ion of paclitaxel is shown in Scheme 1.

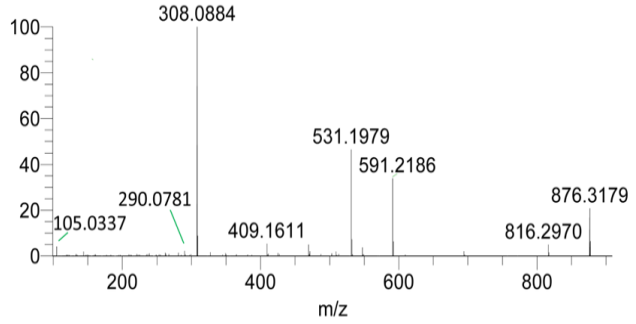

Figure S2. HRMS/MS spectra of the $[M+Na]^+$ ion at *m/z* 876.3207 for paclitaxel.

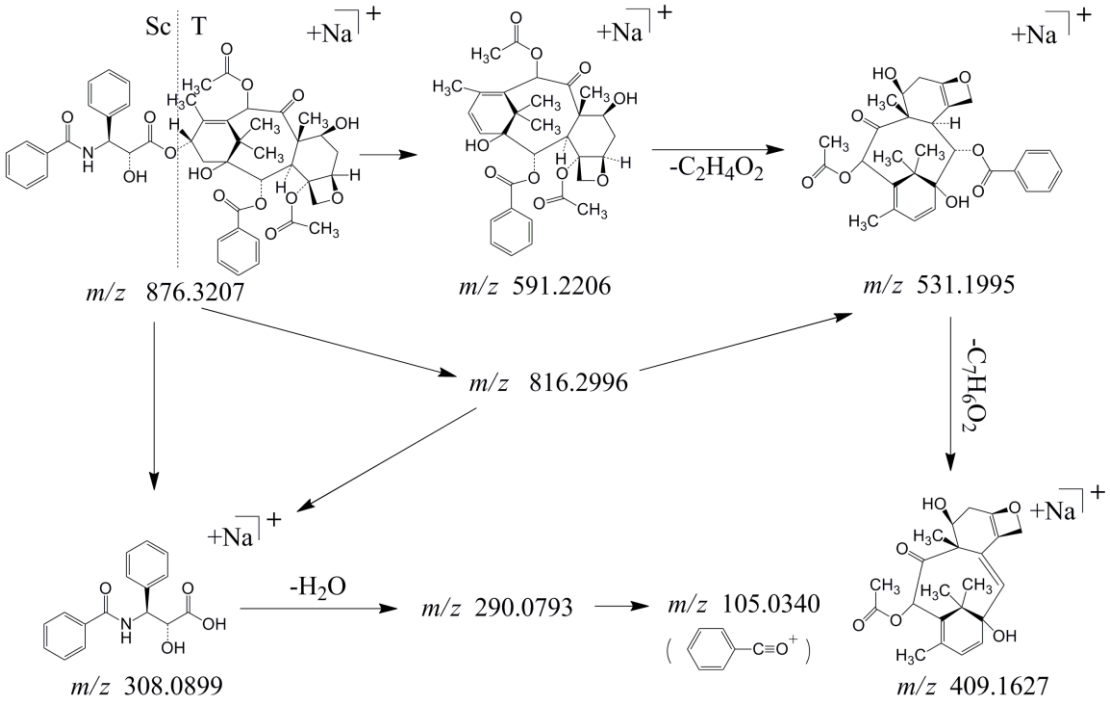

Scheme S1. Fragmentation reaction of the $[M+Na]^+$ ion of paclitaxel.

Structure Elucidation of 10 Metabolites. We identified 10 paclitaxel metabolites in female BALB/c-nu mice that were formed through phase I metabolic processes, such as hydroxylation (M1, M3, M4, M5 and M8), deacetylation (M2), dihydroxylation, dehydration and deacetylation (M7), deacetylation and hydroxylation (M6), hydroxylation and dehydration (M9), and dimethylation (M10). Chemical structures of the 10 metabolites were elucidated based on HRMS/MS, according to structural features of taxoids and metabolites identified in comprehensive study of paclitaxel metabolism.

Four metabolites (M1, M2, M3 and M8), which had been previously detected in mouse, rat, and human, were also identified in our study. For mono-hydroxylated metabolites, as shown in Figure S2, the characteristic ions $[ScH+Na+O]^+$ at *m/z* 324.0848 and $[M+Na-ScH]^+$ at *m/z* 591.2206 were observed in the product ion spectrum of M1, which indicated that hydroxylation occurred at the C3' position. For M1, the assigned positions of hydroxyl groups were confirmed using 3'-hydroxypaclitaxel analytical standards. The characteristic ions $[ScH+Na]^+$ at *m/z* 308.0899, $[M+Na-ScH+O]^+$ at *m/z* 607.2155, and *m/z* 409.1617 indicated that M3 was 2m-hydroxypaclitaxel, whereas characteristic ions at *m/z* 485.1776 and *m/z* 425.1566 indicated that hydroxylation occurred at C6, C16, C17, or C19. Neither M5 nor M8 had the same retention time with 6α-hydroxypaclitaxel analytical standards, and when hydroxylation occurred at C19, the polarity was weaker because of the formation of hydrogen bond. Therefore, M5 and M8 were speculated to be 16(or 17)-hydroxypaclitaxel and 19-hydroxypaclitaxel, respectively. When hydroxylation occurred at the C14 position, adjacent hydroxyl groups increased the possibility of eliminating the hydroxyl as H_2O, so $[M+Na-ScH-2H]^+$ at *m/z* 589.2050 were presented

in HRMS/MS spectra of M9. Because there are two acetyl groups at C10 and C4, we give two possible structures of M2. Furthermore, because its retention time (at 12.63 min) was later than those of M2 and M5, we speculated that M6 was formed by deacetylation at C4 or C10 and hydroxylation at C19. Based on the formation of M6 and M9, a proposed structure of M7 is given. HRMS/MS spectra of M4 displayed characteristic ions, $[ScH+Na+O]^+$ at *m/z* 324.0848 and $[M+Na-ScH+O]^+$ at *m/z* 607.2155, which indicated that M4 was dihydroxypaclitaxel. Because the retention time of M4 (11.30 min) was different from that of 3',6α-dihydroxypaclitaxel (10.13 min), and later than those of M1 and M3, M4 was presumed to be a novel dihydroxypaclitaxel with hydroxylation at C3' and C19 (C16 or C17). For M10, the characteristic ions $[ScH+Na]^+$ at *m/z* 308.0899 and $[M+Na-ScH+2C+4H]^+$ at *m/z* 619.2519 allowed us to propose that M10 is a metabolite resulting from dimethylation at 13-OH and 7-OH.

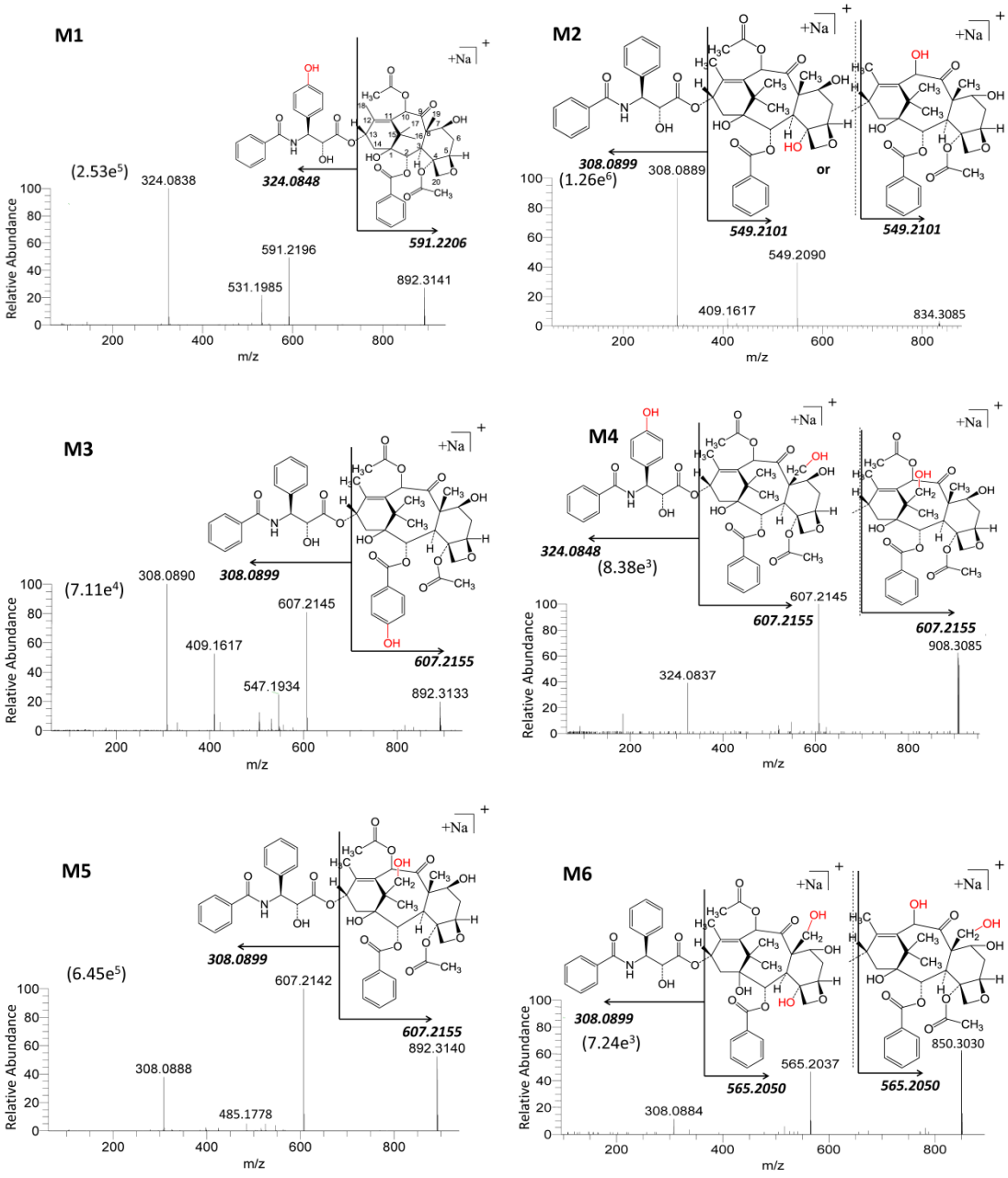

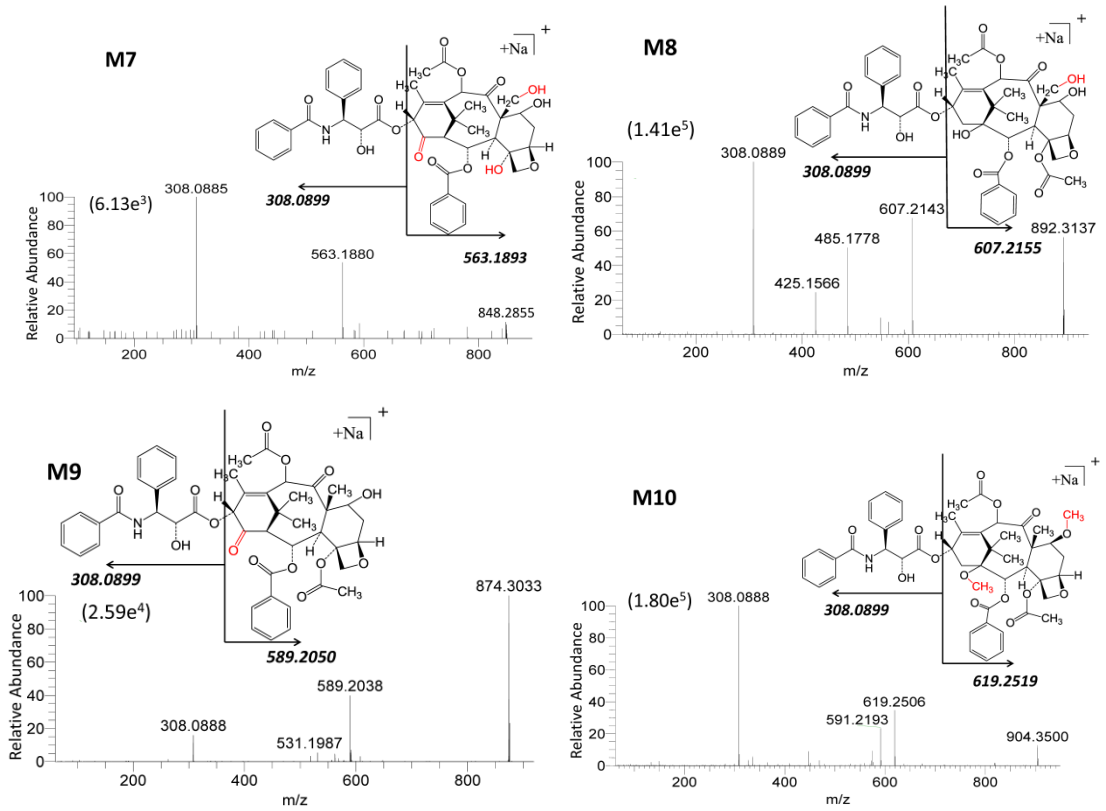

Figure S3. HRMS/MS spectra and proposed structures of M1–M10.

SUPPLEMENTARY REFERENCES

(1) Dromey, R. G.; Stefik, M. J.; Rindfleisch, T. C.; Duffield, A. M. *Analytical Chemistry* **1976**, *48*, 1368-1375.

(2) Halket, J. M.; Przyborowska, A.; Stein, S. E.; Mallard, W. G.; Down, S.; Chalmers, R. A. *Rapid Communications in Mass Spectrometry* **1999**, *13*, 279-284.

(3) Abliz, Z.; Fang, Q. C.; Liang, X. T. *Chinese Science Bulletin* **1999**, *44*, 691-691.